

# *Wld<sup>S</sup>* protects against peripheral neuropathy and retinopathy in an experimental model of diabetes in mice

S. S. Zhu · Y. Ren · M. Zhang · J. Q. Cao · Q. Yang ·  
X. Y. Li · H. Bai · L. Jiang · Q. Jiang · Z. G. He ·  
Q. Chen

Received: 27 February 2011 / Accepted: 31 May 2011 / Published online: 8 July 2011  
© Springer-Verlag 2011

## Abstract

**Aims/hypothesis** We aimed to evaluate the effect of the mutant *Wld<sup>S</sup>* (slow Wallerian degeneration; also known as *Wld*) gene in experimental diabetes on early experimental peripheral diabetic neuropathy and diabetic retinopathy.

**Methods** The experiments were performed in four groups of mice: wild-type (WT), streptozotocin (STZ)-induced diabetic WT, C57BL/*Wld<sup>S</sup>* and STZ-induced diabetic C57BL/*Wld<sup>S</sup>*. In each group, intraperitoneal glucose and insulin tolerance tests were performed; blood glucose, glycated haemoglobin and serum insulin were monitored. These mice were also subjected to the following behavioural tests: grasping test, hot-plate test and von Frey aesthesiometer

test. For some animals, sciatic–tibial motor nerve conduction velocity, tail sensory nerve conduction velocity and eye pattern electroretinogram were measured. At the end of the experiments, islets were isolated to detect glucose-stimulated insulin secretion, ATP content and extent of apoptosis. The NAD/NADH ratio in islets and retinas was evaluated. Surviving retinal ganglion cells were estimated by immunohistochemistry.

**Results** We found that the *Wld<sup>S</sup>* gene is expressed in islets and protects beta cells against multiple low doses of STZ by increasing the NAD/NADH ratio, maintaining the ATP concentration, and reducing apoptosis. Consistently, significantly higher insulin concentrations, lower blood glucose concentrations, and better glucose tolerance were observed in *Wld<sup>S</sup>* mice compared with WT mice after STZ treatment. Furthermore, *Wld<sup>S</sup>* alleviated abnormal sensory responses, nerve conduction, retina dysfunction and reduction of surviving retinal ganglion cells in STZ-induced diabetic models.

**Conclusions/interpretation** We provide the first evidence that expression of the *Wld<sup>S</sup>* gene decreases beta cell destruction and preserves islet function in STZ-induced diabetes, thus revealing a novel protective strategy for diabetic models.

**Electronic supplementary material** The online version of this article (doi:10.1007/s00125-011-2226-1) contains peer-reviewed but unedited supplementary material, which is available to authorised users.

S. S. Zhu · M. Zhang · Q. Yang · X. Y. Li · H. Bai · L. Jiang ·  
Q. Chen (✉)  
Atherosclerosis Research Centre, Nanjing Medical University,  
140 Hanzhong Road,  
Nanjing, 210029, People's Republic of China  
e-mail: qichen@njmu.edu.cn

Y. Ren · Q. Jiang  
The Affiliated Eye Hospital of Nanjing Medical University,  
Nanjing, Jiangsu, People's Republic of China

J. Q. Cao  
Key Laboratory of Molecular Interference of Cardiovascular  
Disease, Nanjing Medical University,  
Nanjing, Jiangsu, People's Republic of China

Z. G. He  
Division of Neuroscience, Children's Hospital,  
Harvard Medical School,  
Boston, MA, USA

**Keywords** Diabetic retinopathy · Islet function ·  
NAD/NADH ratio · Peripheral diabetic neuropathy ·  
Type 1 diabetes · *Wld<sup>S</sup>*

## Abbreviations

DR	Diabetic retinopathy
GHb	Glycated haemoglobin
HE	Haematoxylin and eosin
IPGTT	Intraperitoneal glucose tolerance test
IPITT	Intraperitoneal insulin tolerance test

PARP	Poly(ADP-ribose) polymerase
pERG	Pattern electroretinogram
PDN	Peripheral diabetic neuropathy
RGC	Retinal ganglion cell
SMNCV	Sciatic–tibial motor nerve conduction velocity
SIRT1	Sirtuin 1
STZ	Streptozotocin
TSNCV	Tail sensory nerve conduction velocity
WLD <sup>S</sup>	Slow Wallerian degeneration
WT	Wild-type

## Introduction

Type 1 (insulin-dependent) diabetes is a chronic metabolic disorder characterised by a loss of pancreatic islet beta cell mass, decreased serum insulin, and hyperglycaemia. Much of our understanding of the role of the T cell-mediated autoimmune mechanism has come from the use of animal models. Autoreactive T cells produce inflammatory cytokines, which can upregulate Fas expression on beta cells and stimulate production of nitric oxide and reactive oxygen species, inducing caspase-3-dependent apoptotic signalling cascades [1, 2]. With the excessive DNA damage resulting from reactive oxygen species accumulation, poly(ADP-ribose) polymerase (PARP) is highly activated. Continuous PARP activity in the pancreas leads to depletion of its substrate, NAD<sup>+</sup>, to non-physiological levels, energy failure, inhibition of glyceraldehyde-3-phosphate dehydrogenase of glycolysis, inhibition of insulin synthesis, and, in extreme cases, beta cell death [3]. However, there is still a lack of an efficient protective strategy for beta cell loss and its subsequent pathological events.

The C57BL/*Wld<sup>S</sup>* mouse carries a dominant mutation that delays Wallerian degeneration in the distal stump of an injured axon [4, 5]. *Wld<sup>S</sup>* (also known as *Wld*) mutation comprises an 85 kb tandem triplication, which results in overproduction of slow Wallerian degeneration (WLD<sup>S</sup>) protein. This protein is composed of the N-terminal 70 amino acids of ubiquitin fusion degradation protein 2a (UFD2A), a ubiquitin-chain assembly factor, fused to the complete sequence of nicotinamide mononucleotide adenylyltransferase1 (NMNAT1), an enzyme in the NAD biosynthetic pathway that generates NAD [6, 7]. The *Wld<sup>S</sup>* mouse has been shown to have protective properties in different types of neurodegenerative disease models with axonal degeneration [8, 9]. However, whether *Wld<sup>S</sup>* can antagonise diabetes and diabetic neurodegeneration is not yet known. Here, we provide evidence that *Wld<sup>S</sup>* could attenuate experimental diabetes and early experimental peripheral diabetic neuropathy (PDN) and diabetic retinopathy (DR).

## Methods

**Animal model** Homozygous C57BL/*Wld<sup>S</sup>* mutant mice were obtained from the Institute for Nutritional Sciences, Shanghai Institute for Biological Sciences and Chinese Academy of Sciences. In all studies, C57BL/*Wld<sup>S</sup>* mice were genotyped 4 weeks after birth. Eight-week-old male C57BL/6J wild-type (WT) mice and homozygous C57BL/*Wld<sup>S</sup>* mice were housed under a 12 h light/dark cycle under pathogen-free conditions with free access to mouse chow and water. All animal care and use was in accordance with guidelines established by the Research Animal Care Committee of Nanjing Medical University. Diabetes was induced by injecting mice intraperitoneally with 50 mg/kg body weight of streptozotocin (STZ; Sigma, St Louis, MO, USA) dissolved in citrate buffer (pH 5.5) for 5 days or 150 mg/kg body weight for a single high dose. Non-diabetic mice were injected with sodium citrate buffer alone. Animal fasting weight and tail vein blood glucose concentrations were measured 1 week after STZ administration and every other week using the OneTouch Horizon Glucose Monitoring Kit (LifeScan, Milpitas, CA, USA). Only STZ-injected mice with fasting blood glucose concentrations >11.1 mmol/l were included in the diabetic groups.

**Intraperitoneal glucose tolerance test and intraperitoneal insulin tolerance test** Both intraperitoneal glucose tolerance test (IPGTT) and intraperitoneal insulin tolerance test (IPITT) were carried out on day 9. Mice were fasted for 16 h (IPGTT) or 6 h (IPITT), injected intraperitoneally with D-glucose at 1 g/kg body weight (IPGTT) or with insulin at 0.75 U/kg body weight (IPITT). Blood glucose was analysed at 0, 30, 60 and 120 min after the injection. IPGTT and IPITT were performed on different sets of mice to prevent unnecessary repetitive stress that could interfere with measurements.

**Islet isolation** Male mice were anaesthetised using 10–20% urethane. The peritoneal cavity was opened. Ice-cold collagenase (type V; Sigma; 1 mg/ml in Hank's balanced salt solution) was injected through a catheter introduced into the part of the bile duct running from the liver to the pancreas (2 ml/mouse). Then the filled pancreas was extracted and digested in a water-bath at 37°C for 28 min, purified using a Histopaque gradient separation method, and the islets were hand picked under the Zeiss microscope. Freshly isolated islets were transferred to sterile six-well plates and cultured in RPMI-1640 (Gibco, Shanghai, China) supplemented with 10% FCS (Gibco), 100 U/ml penicillin and 100 µg/ml streptomycin. The islets were allowed to equilibrate for 3 h, after which they were counted, repacked into six-well plates and cultured overnight at 37°C in humidified air with 5% CO<sub>2</sub> for further studies.

**RNA extraction, reverse transcription and gene expression** Spinal cords from mice were flash frozen in liquid nitrogen, and mRNAs of isolated islets and spinal cords were extracted using the RNAiso Plus (Takara, Dalian, China). mRNA was transformed into cDNA using the Prime Script RT reagent kit (Takara); RT-PCR was performed to identify *Wld<sup>S</sup>* gene expression. The following primer sequences were used: *Wld* forward, 5'-CGTTGGCTCTAAGGACAGCAC-3'; *Wld* reverse, 5'-CTGCAGCCCCACCCCTT-3'. *Gapdh* was used as a control gene.

**Glucose-stimulated insulin secretion** After overnight culture, islets were washed and preincubated for 1 h at 37°C in KRB/HEPES buffer supplemented with 0.2% BSA, followed by a 1 h incubation in KRB/HEPES buffer supplemented with 0.2% BSA and in the presence of 3.3 or 16.7 mmol/l glucose. Insulin released during the hour was measured with a radioimmunoassay kit (Bnibt, Beijing, China) following the manufacturer's instructions. The lower limit of the assays was 34.725 pmol/l with a variation coefficient of 10% within the assays and 15% between the assays.

**NAD/NADH assay** Islets or frozen retinas were extracted by two freeze/thaw cycles or homogenisation in 400 µl NAD/NADH Extraction Buffer (BioVision, Mountain View, CA, USA). The homogenate was filtered using 10 kDa cut-off filters. The assay was conducted following the manufacturer's instructions.

**ATP evaluation** ATP concentrations were measured using a luciferase–luciferin ATP Assay Kit (Beyotime, Haimen, China) following the manufacturer's instructions. Protein concentration of the islets was determined using the BCA protein assay, and ATP was normalised to the protein content, expressed as relative luminescence units (RLU)/mg protein.

**Western blotting analysis for caspase 3** Isolated islets were homogenised in protein lysis buffer containing 10% phosphatase inhibitors. Proteins (20–50 µg) were separated by 10% SDS-PAGE (wt/vol.), transferred to poly(vinylidene difluoride) membranes, and probed overnight at 4°C with primary antibodies against caspase 3 (Cell Signal, Boston, MA, USA) and β-actin (Santa Cruz Biotechnology, Santa Cruz, CA, USA). Detection was performed using horseradish peroxidase-labelled anti-rabbit IgG or horseradish peroxidase-labelled anti-mouse IgG and developed with Super-Signal chemiluminescent substrate (Pierce Biotechnology, Rockford, IL, USA).

**Tissue harvest** Pancreas was harvested 9 weeks after induction of diabetes, then embedded in paraffin. Sections

(5 µm thick) were cut and stained with haematoxylin and eosin (HE). Before the mice were killed, a blood sample (1 ml) was collected for measurement of glycated haemoglobin (GHb) and serum insulin. GHb was measured using the VARIANT II Hemoglobin Analyzer (Bio-Rad, Hercules, CA, USA). Serum insulin was measured with a radioimmunoassay kit (Bnibt).

**Determination of muscle strength** Forelimb grip strength was determined using a custom-made automated grip strength meter (YLS-13A; Shandong Academy of Medical Sciences Device Station, Jinan, China). Animals were placed on a platform and allowed to grasp a ring. Mice were pulled away until they released the ring, and the strength was determined with an electronic pull strain gauge. The test was repeated three times on each mouse, and the mean value was calculated as the muscle strength.

**Thermal analgesia** To determine sensitivity to noxious heat, mice were placed individually on the hot-plate instrument (YLS-6B; Shandong Academy of Medical Sciences Device Station). The temperature was set at 55±0.2°C. Brisk withdrawal or hind paw flinching was considered a positive response. The hind paw withdrawal latency in response to heat was recorded. Individual measurements were repeated three times, and the mean value was calculated as the thermal threshold.

**Mechanical analgesia** Mechanical analgesia was evaluated by quantifying the withdrawal threshold of the hind paw in response to mechanical stimulation using a von Frey aesthesiometer (range 0.008–300 g; UgoBasile, Comerio VA, Italy). Mice were placed in individual Plexiglass boxes on a stainless steel mesh floor and were allowed to adjust for at least 30 min. A series of calibrated von Frey filaments was applied perpendicularly to the planter surface of a hind paw with sufficient force to bend the filament for 6 s. Brisk withdrawal or paw flinching was considered a positive response. In the absence of a response, a filament with the next greatest force was applied. In the presence of a response, a filament with the next lowest force was applied. The test was repeated four or five times at 5 min intervals on each animal, and the mean value was used.

**Nerve conduction studies** At 7 weeks after STZ administration, sciatic–tibial motor nerve conduction velocity (SMNCV) and tail sensory nerve conduction velocity (TSNCV) were measured by Powerlab/8 s (AD Instrument, Sydney, NSW, Australia). Mice were anaesthetised with 20% urethane, and body temperature was monitored with a dermal temperature probe and maintained at 37°C with a warming lamp. The needle electrodes were cleaned with 70% alcohol between animals to maintain pathogen-free

status. SMNCV was determined by recording in the dorsum of the foot and stimulating with supramaximal stimulation first at the knee, then at the sciatic notch. Latencies were measured in each case from the initial onset of the compound muscle action potential. Then SMNCV was calculated by dividing the distance between the cathode placements by the difference calculated by subtracting the motor distal latency at the knee from the sciatic notch. TSNCV was determined by recording on the distal tail and stimulating at the two different parts of the proximal tail. It was calculated by dividing the distance between the cathode placements by the difference calculated by subtracting the latency at the two different placements.

**Pattern electroretinogram** Pattern electroretinograms (pERGs) were measured by EP-100 Pro/Multifocal (Tomey, Nagoya, Japan), and were recorded in response to contrast reversal of horizontal black and white square wave gratings with a mean luminance of 50 photopic (ph) cd/m<sup>2</sup>. The standard grating contrast was 90%, with a 1 Hz reversal rate, and spatial frequency of 0.05 cycles/degree. It was displayed on an RGB monitor 28 cm high by 34 cm wide at a distance of 15 cm from the mouse's eye. The spatial frequency and approximate contrast have been reported to maximise pERG amplitude in the mouse.

**Histology and immunohistochemistry** At the completion of ERGs, mice were killed by cervical dislocation. Both eyes were enucleated and fixed in Feteke's solution for 2 h, followed by a 12 h fixation in 10% neutral formaldehyde. After dehydration in a graded ethanol series, eyes were embedded in paraffin. Sections (5 µm thick) were cut along the vertical meridian at 0.05 mm intervals, yielding six sections from each eye with six mice each group. Then the sections were stained with HE. For immunohistochemistry, mouse monoclonal anti-TUJ1 (1:200 dilution; Lifespan Bioscience, Seattle, WA, USA) was used to estimate surviving retinal ganglion cells (RGCs). After deparaffinisation and rehydration with PBS, specimens were incubated with 3% H<sub>2</sub>O<sub>2</sub> for 15 min to reduce the activity of endogenous peroxidase, and then in a solution of PBS containing 5% BSA for 30 min to block non-specific antibody binding. The primary antibody was added to the specimens and incubated overnight at 4°C in a sealed chamber to prevent dehydration. The secondary antibody biotinylated rabbit anti-mouse (1:100 dilution) was applied for 1 h at room temperature. Specimens were then treated with avidin/biotin complex solution, washed with PBS, and incubated with 3,3'-diaminobenzidine substrate for 10 min. Counterstaining was carried out with haematoxylin. The specimens were then dehydrated in 70%, 95%, 100% ethanol. The image was acquired on an Olympus BX51 microscope using an Olympus DP70 digital camera.

Ganglion cell number was quantified from the central (around the optic nerve head) to the peripheral retina by counting the nuclei in the photo images. Surviving (TUJ1<sup>+</sup>) RGCs were identified only if they were located within the ganglion cell layer and had large, round cell bodies with positively stained 3,3'-diaminobenzidine substrate.

**Statistical analysis** Statistical analysis was conducted using GraphPad Prism Software version 5.0. Results are presented as means±SEM. Differences were determined using two-tailed Student's *t* test or ANOVA, with a Newman–Keuls test to determine post hoc differences. Differences were considered significant at a two-tailed *p* value of <0.05.

## Results

***Wld<sup>S</sup> decreased STZ-induced hyperglycaemia and improved islet function*** Under normal conditions, WT and *Wld<sup>S</sup>* mice showed equivalent concentrations of fasting blood glucose. When they were treated with multiple low-dose STZ (5×50 mg/kg), the fasting blood glucose of STZ-injected WT mice began to increase on day 3, and all STZ-injected WT mice had developed hyperglycaemia (≥11.1 mmol/l) 2 days after the final injection, whereas only 33.3% of STZ-treated *Wld<sup>S</sup>* mice were hyperglycaemic (Fig. 1a). Consistently, the results of IPGTT performed on day 9 as an in vivo measure of beta cell function showed that STZ-induced glucose intolerance was significantly ameliorated in *Wld<sup>S</sup>* mice (Fig. 1b). However, IPITT showed that *Wld<sup>S</sup>* did not alter insulin sensitivity (Fig. 1c). Furthermore, islets isolated from WT and *Wld<sup>S</sup>* mice showed a similar level of insulin release in response to glucose stimulation. The STZ treatment significantly decreased insulin release from the WT islets. However, this impairment was abrogated in *Wld<sup>S</sup>* islets (Fig. 1d). Then only STZ-injected mice with fasting blood glucose concentrations >11.1 mmol/l were included in the diabetic groups. Typical symptoms of diabetes include polydipsia, polyuria and weight loss. All diabetic mice had significantly higher fasting blood glucose concentrations than vehicle-injected mice; this difference was maintained throughout the study (Fig. 2a). The non-diabetic mice had increasing body weight during the whole study, while diabetic mice exhibited a loss of body weight or a reduction in body weight gains (electronic supplementary material [ESM] Fig. 1). The fasting serum insulin concentrations of the diabetic mice were significantly reduced compared with those in the control group (Fig. 2b). Conversely, the GHb concentrations of the diabetic mice were significantly raised after STZ injection (Fig. 2c). *Wld<sup>S</sup>* also partially corrected the STZ-induced increase in blood glucose concentration and decrease in serum insulin concentration in the diabetic mice

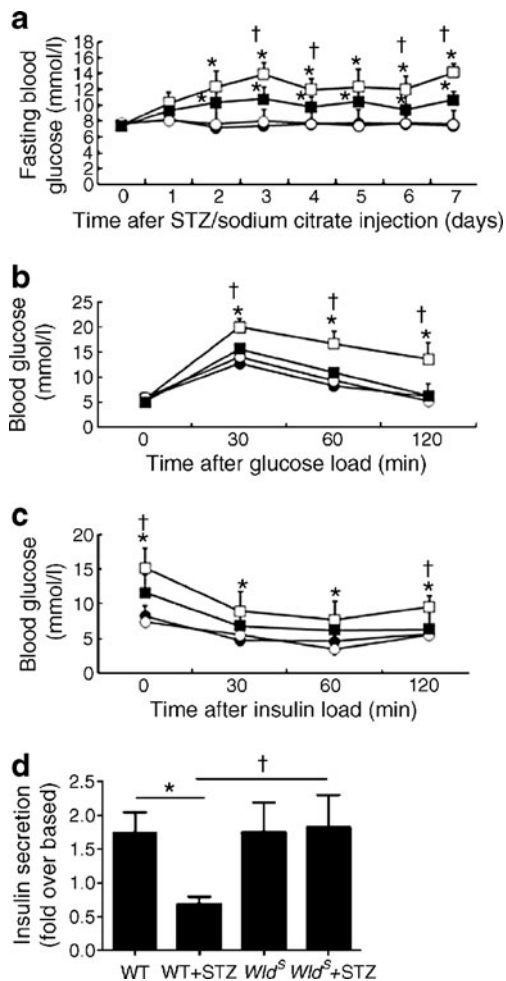


**Fig. 1** **a** Fasting blood glucose concentrations during and after multiple low doses of STZ. *Wld<sup>S</sup>* mice (black squares) had a significantly lower fasting blood glucose concentration than WT mice (white squares) after STZ treatment. No significant difference was detected between control groups (black circles, WT mice; white circles, *Wld<sup>S</sup>* mice). **b** IPGTT was conducted by injecting D-glucose (1 g/kg body weight) 5 days after STZ treatment. Glucose clearance was significantly improved in *Wld<sup>S</sup>* mice (black squares) compared with WT mice (white squares) and no difference was found between control groups (black circles, WT mice; white circles, *Wld<sup>S</sup>* mice). **c** IPITT was conducted by injecting insulin (0.75 U/kg body weight) 5 days after STZ treatment. Blood glucose concentrations were measured at the indicated times. It revealed that *Wld<sup>S</sup>* did not alter the insulin sensitivities (white squares, WT mice; black squares, *Wld<sup>S</sup>* mice) and no difference was found between control groups (black circles, WT mice; white circles, *Wld<sup>S</sup>* mice). **d** Glucose-stimulated insulin release after treatment with STZ for 5 days. Insulin release in response to 16.7 mmol/l glucose was significantly impaired in STZ-treated WT islets compared with WT control. It was well preserved in STZ-treated *Wld<sup>S</sup>* islets. Values are expressed as means±SEM,  $n=6$  per group. \* $p<0.05$  compared with control group. † $p<0.05$  compared with STZ-treated WT mice

(Fig. 2a–c). Nine weeks after STZ treatment, all groups of mice were killed. HE staining of non-STZ-treated WT and *Wld<sup>S</sup>* pancreas showed normal distribution. Diabetic WT mice showed dramatic islet destruction. In contrast, STZ-treated *Wld<sup>S</sup>* mice showed large, round islets (Fig. 3). These

results suggest that *Wld<sup>S</sup>* protected beta cells against insult by multiple low doses of STZ.

*Wld<sup>S</sup> improved beta cell survival after STZ treatment* Although numerous reports have shown that the *Wld<sup>S</sup>* gene is expressed in neuronal tissue, it is unknown whether it is also expressed in islets. By RT-PCR, we found that *Wld<sup>S</sup>* is also expressed in the islets of *Wld<sup>S</sup>* mice (Fig. 4a). In separate experiments, we found that *Wld<sup>S</sup>* ameliorated the decreased NAD/NADH ratio (Fig. 4b), ATP depletion (Fig. 4c) and activated caspase response (Fig. 4d, e) in the islets triggered by STZ administration.

*Wld<sup>S</sup> improved the lifespan of diabetic mice* To further determine the effect of *Wld<sup>S</sup>* in diabetic complications excluding the factor of blood glucose, we used a single high dose (150 mg/kg) of STZ to induce diabetes. These diabetic mice had similar fasting blood glucose concentrations (Fig. 5a) as well as serum insulin concentrations and GHb concentrations (Fig. 5c, d). Interestingly, *Wld<sup>S</sup>* mice showed remarkably improved lifespan response to STZ-induced diabetes. Three weeks after STZ administration, the survival rate of WT mice was 49%, while the lifespan of *Wld<sup>S</sup>* mice was 86%. The effects of *Wld<sup>S</sup>* on the lifespan of diabetic mice was maintained 7 weeks after induction, when 81% of the *Wld<sup>S</sup>* animals, but only 31% of the WT animals, survived.

*Wld<sup>S</sup> alleviated diabetes-induced neuropathy* In these animals, we also examined other diabetic consequences. Although diabetic mice displayed reduced muscle strength during the experiment, there was no significant difference between STZ-treated WT and *Wld<sup>S</sup>* mice (Fig. 6a). Diabetic mice with a 7 week duration of STZ-induced diabetes had clearly manifested thermal hypoalgesia detected by measuring the latencies of hind paw withdrawal. There was no statistically significant difference between STZ-treated WT and *Wld<sup>S</sup>* mice during the 7 weeks (Fig. 6b). Diabetic mice with 7-week duration of STZ-induced diabetes also had mechanical hypoalgesia detected with a von Frey aesthesiometer by measuring paw withdrawal thresholds in response to noxious stimulation with rigid von Frey filaments. The paw withdrawal thresholds were increased by 88.89% in diabetic WT mice compared with controls 3 weeks after STZ injection ( $p<0.05$ ), and gradually increased 1.46-fold in diabetic WT mice compared with controls 7 weeks after STZ injection ( $p<0.05$ ). *Wld<sup>S</sup>* partially ( $p<0.05$  vs controls and  $p<0.05$  vs WT diabetic group) corrected the diabetes-induced increase in paw withdrawal thresholds (Fig. 6c). According to the Animal Models of Diabetic Complications Consortium (AMDC), electrophysiological measures of nerve impairment are the ‘gold standard’ for determining sensory and motor nerve function and

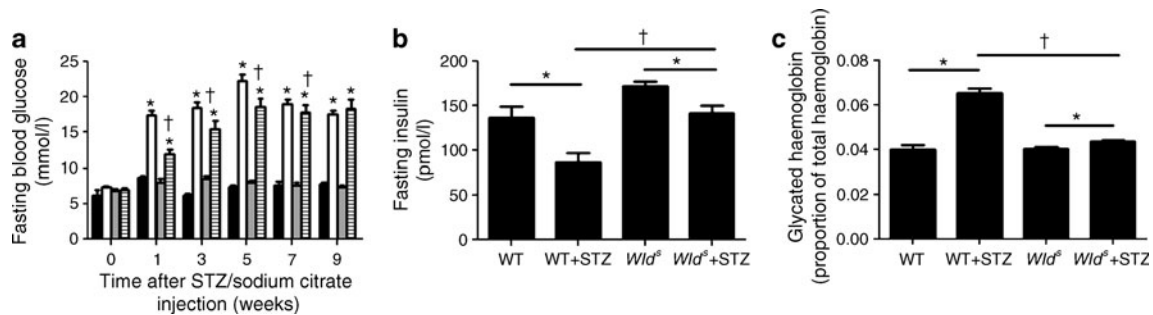


**Fig. 2** Metabolic variables in mice during induction/onset of diabetes with multiple low doses of STZ. **a** Fasting tail vein blood glucose concentrations were measured 1 week after STZ and every other week. Fasting serum insulin (**b**) and GHb (**c**) concentrations were measured 9 weeks after induction of diabetes. Values are expressed as

means±SEM,  $n=5-20$  per group. Black bar, WT mice; white bar, STZ-treated WT mice; grey bar, *Wld<sup>S</sup>* mice; striped bar, STZ-treated *Wld<sup>S</sup>* mice. \* $p<0.05$  compared with control group. † $p<0.05$  compared with STZ-treated WT mice

include assessment of TSNCV and SMNCV [10]. At 7 weeks after STZ administration, SMNCV in WT diabetic mice was reduced by 54.04% compared with the controls ( $p<0.05$ ), and in *Wld<sup>S</sup>* diabetic mice the reduction was 18.75% ( $p<0.05$ ; Fig. 7a). TSNCV in WT diabetic mice was reduced by 43.44% compared with the controls ( $p<0.05$ ), and in *Wld<sup>S</sup>* diabetic mice the reduction was 12.85% ( $p<0.05$ ; Fig. 7b). Thus, *Wld<sup>S</sup>* has significant effects on SMNCV and TSNCV deficits ( $p<0.05$  vs WT diabetic group).

*Wld<sup>S</sup> alleviated diabetes-induced retinopathy* Diabetes can damage non-vascular cells of the retina, resulting in alterations in function and loss of RGCs, horizontal cells, amacrine cells and photoreceptors [11, 12]. We detected the ERG response to contrast reversal of horizontal black and white square wave bar at 7 weeks after STZ administration.

Representative waveforms are shown in Fig. 7c–f. The peak amplitude of the wave was significantly decreased by 79.71% in the STZ-treated WT group compared with the control group, whereas the STZ-treated *Wld<sup>S</sup>* group showed no significant reduction (Fig. 7g). After 7 weeks of hyperglycaemia, cell body numbers in the ganglion cell layer were decreased by 25.98%, and surviving RGCs were decreased by 17.11% in WT diabetic mice, whereas the STZ-treated *Wld<sup>S</sup>* group showed no significant reduction (Fig. 8c, d). The NAD/NADH ratio in WT diabetic retina was decreased dramatically, and *Wld<sup>S</sup>* ameliorated this reduction (Fig. 8e).

## Discussion

Although the protective effects of *Wld<sup>S</sup>* against axonal degeneration have been well documented [13–17], our

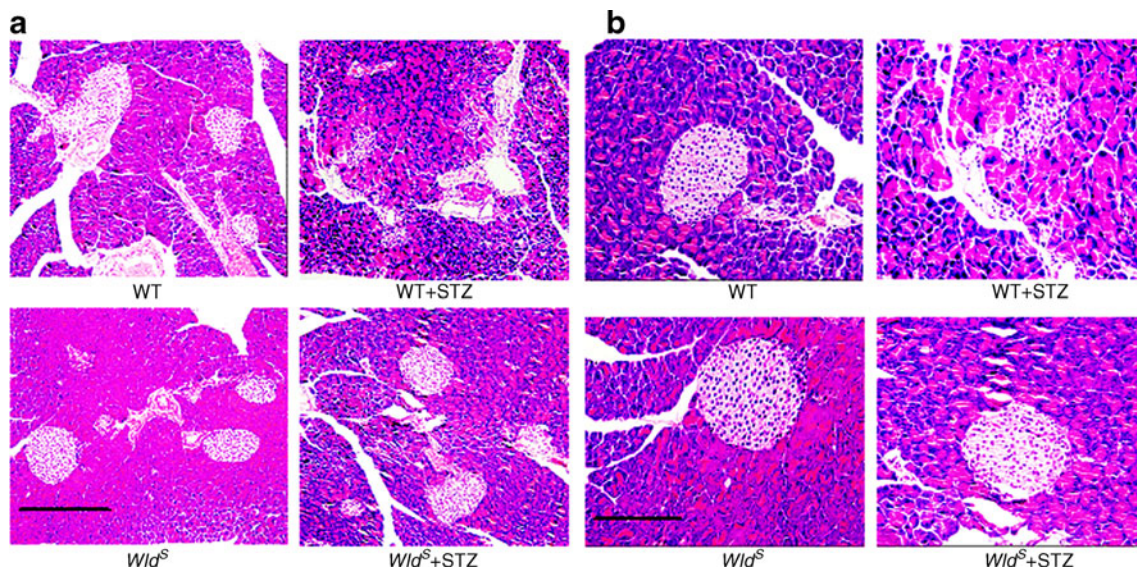


**Fig. 3** Pancreas was harvested 9 weeks after induction of diabetes. Representative microphotographs of HE staining of pancreas in control and diabetic mice are shown. **a** Original magnification,  $\times 200$ ; scale bar, 12.5  $\mu\text{m}$ . **b** Original magnification,  $\times 400$ ; scale bar, 6.3  $\mu\text{m}$

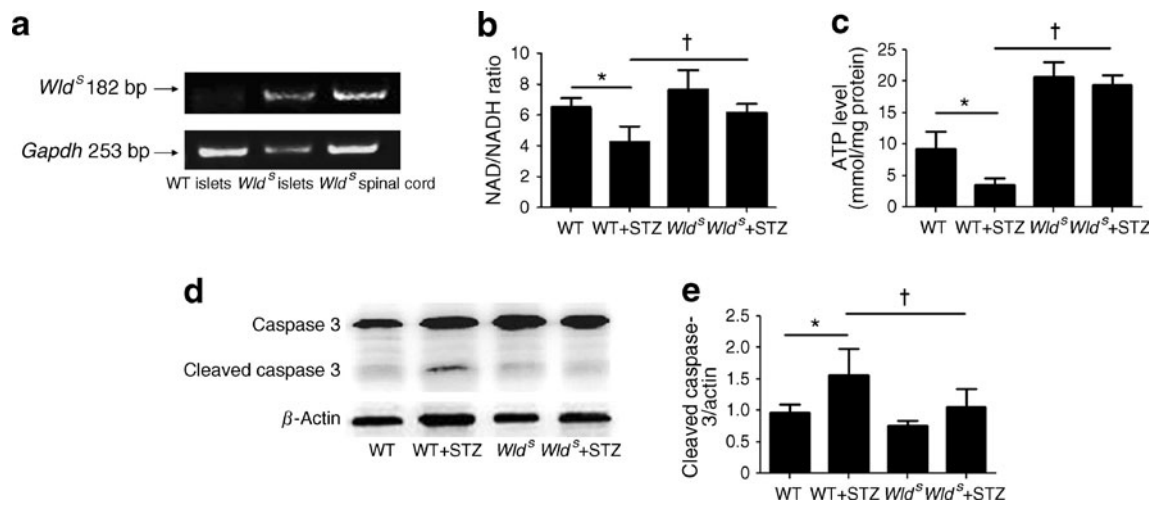


**Fig. 4** **a** Expression of *Wld<sup>S</sup>* in *Wld<sup>S</sup>* mouse islets was identified by RT-PCR. The RT-PCR product amplified from *Wld<sup>S</sup>* mouse spinal cord was used as a positive control. **b** NAD/NADH ratio in islets from control and diabetic mice. **c** ATP concentrations in islets from control and diabetic mice were determined by luminometry using the

luciferin–firefly luciferase reaction. **d** Western blot analysis of caspase-3 using islet lysates from control and diabetic mice, with a representative immunoblot. **e** Densitometric analysis of three different immunoblots using Image-J software. \* $p < 0.05$  compared with control group. † $p < 0.05$  compared with STZ-treated WT mice

studies provide evidence that it can protect against STZ-triggered pancreatic beta cell death and subsequent diabetic symptoms and pathological events in mice. *Wld<sup>S</sup>* is expressed in islets, suggesting a direct protective effect on beta cells. In addition, *Wld<sup>S</sup>* might also show beta cell-independent protection of axons in both the peripheral nervous system and central nervous system. Consistent with this, we found that *Wld<sup>S</sup>* could prevent STZ-triggered nerve conduction deficits, indicated by measurements of the TSNCV and SMNCV. Interestingly, we found that *Wld<sup>S</sup>* diabetic mice have reduced mechanical hypoalgesia, but thermal hypoalgesia was not affected. This may reflect differential sensitivity of large myelinated vs small unmyelinated fibres in this animal model [18]. In addition to the peripheral nervous system, *Wld<sup>S</sup>* also showed protective effects against diabetic neuropathy in the retina, as indicated

by significant improvement in the oscillatory potentials of the electroretinogram, which is considered to be a functional indicator of inner retinal neurotransmission [11].

The mechanisms of *Wld<sup>S</sup>* protection of beta cells and axons in STZ-triggered diabetic models remain to be determined. Previous studies have suggested that *Wld<sup>S</sup>* protects axons and synapses in both the central and peripheral nervous systems from injury, neurotoxin and inherited neurodegenerative conditions. Such protective effects of *Wld<sup>S</sup>* depend on the NAD-synthesising enzymatic activity of nicotinamide mononucleotide adenylyltransferase-1, a major component of the WLD<sup>S</sup> fusion protein. Recent studies have suggested that it is the WLD<sup>S</sup> protein in the cytoplasmic compartment, in particular those associated with mitochondria, that is responsible for the protective effects. NAD is well known as a coenzyme in

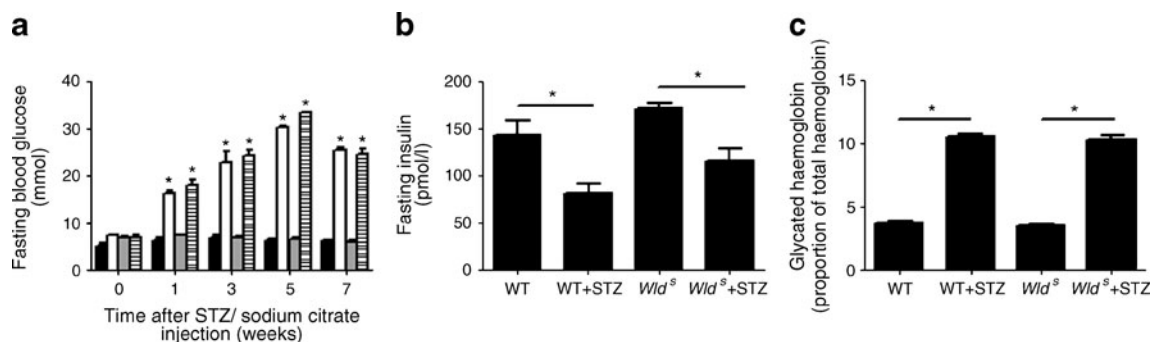


**Fig. 5** Metabolic variables in mice during induction/onset of diabetes with a single high dose (150 mg/kg) of STZ. **a** Fasting tail vein blood glucose concentrations were measured 1 week after STZ and every other week. Fasting serum insulin (**b**) and GHb (**c**) concentrations were measured 7 weeks after induction of diabetes. No significant

difference was detected between STZ-treated WT and *Wld<sup>S</sup>* mice. Values are expressed as means±SEM,  $n = 5–20$  per group. Black bar, WT mice; white bar, STZ-treated WT mice; grey bar, *Wld<sup>S</sup>* mice; striped bar, STZ-treated *Wld<sup>S</sup>* mice. \* $p < 0.05$  compared with control group

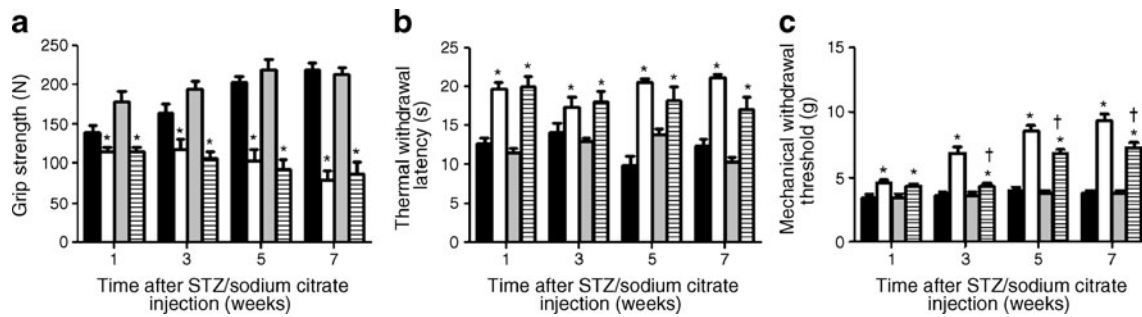


**Fig. 6** Behavioural tests were measured 1 week after STZ and every other week. **a** Grip strength in diabetic and control mice. **b** Paw withdrawal latencies in response to thermal stimuli in control and diabetic mice. **c** Paw withdrawal thresholds in response to stimulation with rigid von Frey filaments in control and diabetic mice. Values are

expressed as means±SEM,  $n=5-14$  per group. Black bar, WT mice; white bar, STZ-treated WT mice; grey bar, *Wld<sup>S</sup>* mice; striped bar, STZ-treated *Wld<sup>S</sup>* mice. \* $p<0.05$  compared with control group. † $p<0.05$  compared with STZ-treated WT mice

oxidation–reduction reactions, in which it can accept and donate electrons and participate in ATP generation. Thus, it is possible that WLD<sup>S</sup>-mediated protection against beta cell death is due to similar mechanisms. Previous studies have shown that intracellular events that affect NAD concentrations or NAD/NADH ratios may affect physiological and pathological processes through sirtuin 1 (SIRT1)-dependent pathways [8, 9]. SIRT1, which is constitutively produced in the endocrine cells of the islets of Langerhans, can repress uncoupling protein 2, enhancing ATP production and thereby sensitising the pancreas to blood glucose [19, 20]. Moreover, nicotinamide (vitamin B<sub>3</sub>), a water-soluble vitamin, is a major NAD<sup>+</sup> precursor, a product inhibitor of most of the NAD<sup>+</sup>-consuming enzymes, and a weak first-generation inhibitor of PARP [21]. It has been the subject of intensive clinical trials around the world as a means of preventing or delaying the clinical onset of diabetes in humans [22, 23]. Other structurally diverse PARP inhibitors, such as 3-aminobenzamide and PJ34 (the hydrochloride salt of *N*-[oxo-5,6-dihydrophenanthridin-2-yl]-*N,N*-

dimethylacetamide), as well as PARP deficiency (*Parp*<sup>-/-</sup>) also attenuated hyperglycaemia and decreased NAD<sup>+</sup> concentrations of beta cells and consequently prevented their destruction [24–26]. These inhibitors, as well as *Parp*<sup>-/-</sup> mice, were also protected from diabetic SMNCV and TSNCV deficits, neurovascular dysfunction and nerve energy failure, which were clearly manifest in the WT (*Parp*<sup>+/+</sup>) diabetic mice [18, 27, 28]. Other studies have revealed that PARP activation is present in RGC layers of rats with short-term (4 weeks) STZ diabetes [29]. In rats with 12-week STZ diabetes, increased poly(ADP-ribose) reactivity is present in the nuclei of the ganglion cell layer [30]. 3-Aminobenzamide and PJ34 blunted it, and this was associated with a reduction in retinal NAD<sup>+</sup> concentration [29, 30]. Thus, a possible model is that *Wld<sup>S</sup>* prevents development of type 1 diabetes by preventing intracellular NAD<sup>+</sup> consumption and decreases in the ATP pool, inhibiting beta cell apoptosis; and it is supposed that *Wld<sup>S</sup>* attenuates early PDN and DR probably by increasing NAD biosynthesis and partial inhibition of PARP.

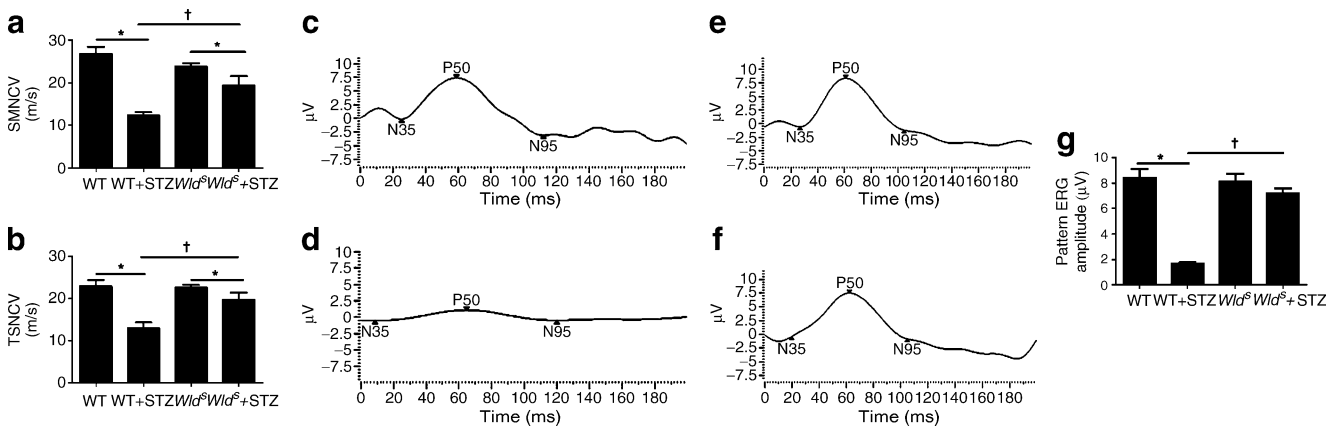


**Fig. 7** SMNCV **a** and TSNCV **b** measured in ms were quantified in control and diabetic mice 7 weeks after STZ. **c–f** Representative pERG waveforms from control and diabetic mice at the 7 week time point (**c** WT; **d** WT + STZ; **e** *Wld<sup>S</sup>*; **f** *Wld<sup>S</sup>* + STZ). **g** Peak amplitudes

of the response wave in control and diabetic mice. For **a**, **b** and **g**, values are expressed as means±SEM,  $n=5-9$  per group. \* $p<0.05$  compared with control group. † $p<0.05$  compared with STZ-treated WT mice



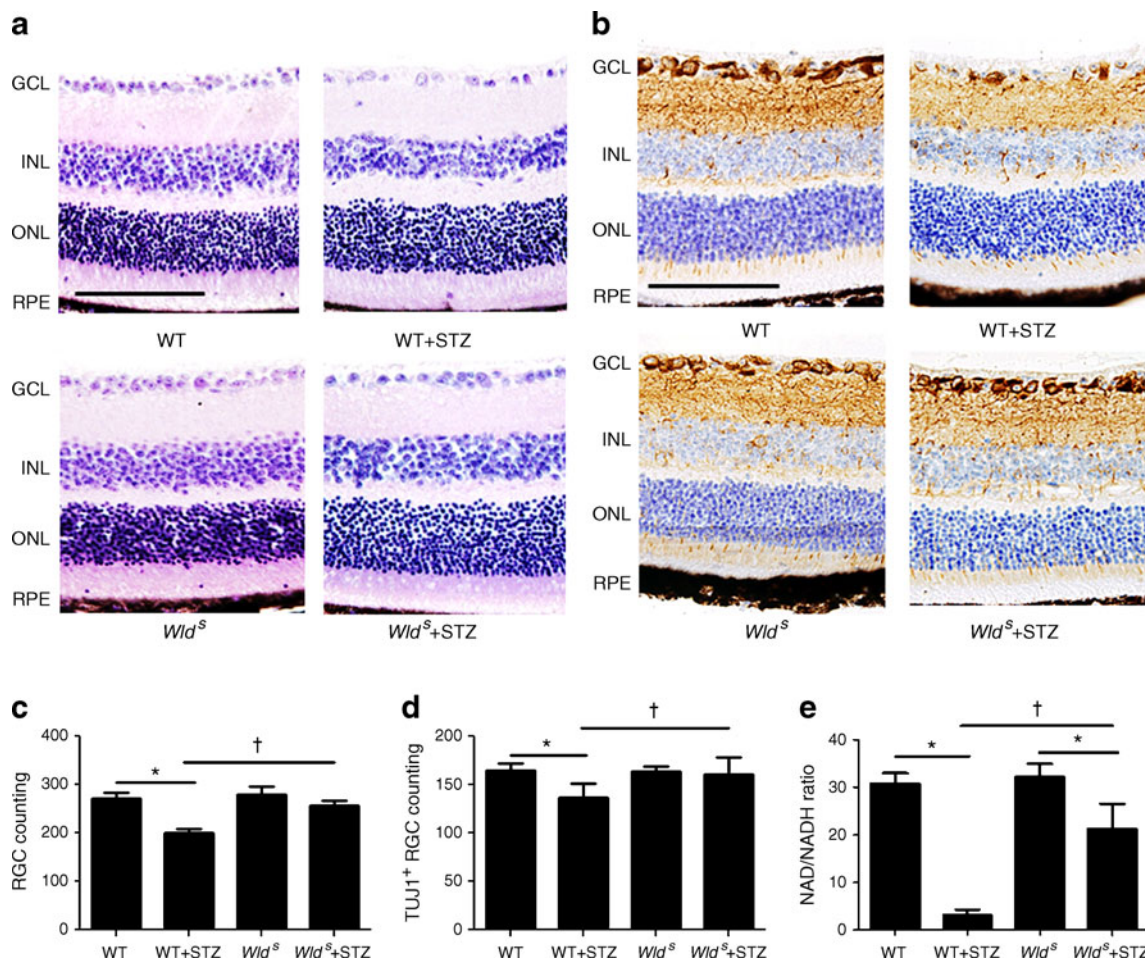


**Fig. 8** Eyes were harvested 7 weeks after induction of diabetes. **a, b** Representative microphotographs of HE and immunohistochemistry staining of retinas in control and diabetic mice. Retina shows the presence of all retinal layers; GCL, ganglion cell layer; INL, inner nuclear layer; ONL, outer nuclear layer; RPE, retinal pigment epithelium layer. Original magnification,  $\times 400$ ; scale bar,  $6.3 \mu\text{m}$ . **c**,

**d** RGC and TUJ1<sup>+</sup> RGC count in retinas from control and diabetic mice. **e** NAD/NADH ratio in retinas from control and diabetic mice. For **c–e**, values are expressed as mean $\pm$ SEM,  $n=5–9$  per group. \* $p<0.05$  compared with control group. † $p<0.05$  compared with STZ-treated WT mice

Diabetes-induced damage to peripheral nerves culminates in development of diabetic distal symmetric sensorimotor polyneuropathy, typically referred to as PDN [31]. Diabetes may reduce insulin receptor signalling in the retina, leading to neurodegeneration. Neuroretinal compromise may develop early in the course of DR, even before the onset of microvascular changes [32]. DR may be a sensory neuropathy which affects the retinal parenchyma, similarly to PDN. Hyperglycaemia leads to diabetic complications via multiple mechanisms, which contribute to enhanced oxidative/nitrosative stress, which is in turn responsible for activation of important downstream pathways, e.g. mitogen-activated protein kinases, inflammatory response and PARP. Growing evidence indicates that catalytic activation of PARP is an early and fundamental mechanism of diabetic complications [33, 34]. PARP activation causes: (1) NAD<sup>+</sup> depletion and energy failure [35, 36]; (2) changes in transcriptional regulation and gene

expression [37, 38]; (3) diversion of the glycolytic flux from glyceraldehyde-3-phosphate dehydrogenase to several pathways associated with hyperglycaemia-induced injury [39]; and (4), in extreme cases, induction of necrosis and apoptosis [36, 40].

It is well known that diabetic rodents have a limited lifespan. In the last decade, a direct relationship between SIRT1 and life extension has been shown in lower organisms such as yeast, *Caenorhabditis elegans* and *Drosophila melanogaster* [41–43]. *Wld<sup>S</sup>* may improve lifespan response to STZ-induced diabetes by maintaining NAD<sup>+</sup> concentrations and activation of SIRT1.

In conclusion, these data suggest that *Wld<sup>S</sup>* decreases beta cell destruction and preserves islet function in STZ-induced diabetes, and it may be protective against neuronal pathology associated with diabetic models. These results suggest a novel protective strategy for diabetic models and perhaps patients.

**Acknowledgements** This work was supported by project grants from the National Natural Science Foundation of China to Q. Chen (no. 30730044, no. 81070120) and Z. G. He (no. 30628017) and a project grant from the Science Foundation of Nanjing Medical University (no. 06NMU2007) to L. Jiang.

S.S.Z. was responsible for the conception and design of the study, the analysis and interpretation of data, and drafting the article and revising it critically; Y.R. was responsible for the design of the study, the analysis of data and revising the manuscript. M.Z., Q.Y, H.B., Q.J. and X.Y.L. were responsible for the analysis of data and revising the manuscript. J.Q.C. and L.J. were responsible for the conception and design of the study and revising the manuscript. Z.G.H. was responsible for the interpretation of data and revising the manuscript. Q.C. was responsible for the conception and design of the study, the interpretation of data, and revising the manuscript. All authors gave final approval.

**Duality of interest** The authors declare that there is no duality of interest associated with this manuscript.

## References

1. Yoon JW, Jun HS (2005) Autoimmune destruction of pancreatic beta cells. *Am J Ther* 12:580–591
2. Ryan A, Murphy M, Godson C, Hickey FB (2009) Diabetes mellitus and apoptosis: inflammatory cells. *Apoptosis* 14:1435–1450
3. Charron MJ, Bonner-Weir S (1999) Implicating PARP and NAD<sup>+</sup> depletion in type I diabetes. *Nat Med* 5:269–270
4. Lunn ER, Perry VH, Brown MC, Rosen H, Gordon S (1989) Absence of Wallerian degeneration does not hinder regeneration in peripheral nerve. *Eur J Neurosci* 1:27–33
5. Glass JD, Brushart TM, George EB, Griffin JW (1993) Prolonged survival of transected nerve fibres in C57BL/Ola mice is an intrinsic characteristic of the axon. *J Neurocytol* 22:311–321
6. Conforti L, Tarlton A, Mack TG et al (2000) A Ufd2/D4Cole1e chimeric protein and overexpression of Rbp7 in the slow Wallerian degeneration (WldS) mouse. *Proc Natl Acad Sci USA* 97:11377–11382
7. Mack TG, Reiner M, Beirowski B et al (2001) Wallerian degeneration of injured axons and synapses is delayed by a Ube4b/Nmnat chimeric gene. *Nat Neurosci* 4:1199–1206
8. Araki T, Sasaki Y, Milbrandt J (2004) Increased nuclear NAD biosynthesis and SIRT1 activation prevent axonal degeneration. *Science* 305:1010–1013
9. Wang J, Zhai Q, Chen Y et al (2005) A local mechanism mediates NAD-dependent protection of axon degeneration. *J Cell Biol* 170:349–355
10. Sullivan KA, Hayes JM, Wiggin TD et al (2007) Mouse models of diabetic neuropathy. *Neurobiol Dis* 28:276–285
11. Kern TS, Barber AJ (2008) Retinal ganglion cells in diabetes. *J Physiol* 586:4401–4408
12. Sasaki M, Ozawa Y, Kurihara T et al (2010) Neurodegenerative influence of oxidative stress in the retina of a murine model of diabetes. *Diabetologia* 53:971–979
13. Gillingwater TH, Ingham CA, Parry KE et al (2006) Delayed synaptic degeneration in the CNS of Wlds mice after cortical lesion. *Brain* 129:1546–1556
14. Sajadi A, Schneider BL, Aebischer P (2004) Wlds-mediated protection of dopaminergic fibers in an animal model of Parkinson disease. *Curr Biol* 14:326–330
15. Samsam M, Mi W, Wessig C et al (2003) The Wlds mutation delays robust loss of motor and sensory axons in a genetic model for myelin-related axonopathy. *J Neurosci* 23:2833–2839
16. Ferri A, Sanes JR, Coleman MP, Cunningham JM, Kato AC (2003) Inhibiting axon degeneration and synapse loss attenuates apoptosis and disease progression in a mouse model of motoneuron disease. *Curr Biol* 13:669–673
17. Gillingwater TH, Haley JE, Ribchester RR, Horsburgh K (2004) Neuroprotection after transient global cerebral ischemia in Wld(s) mutant mice. *J Cereb Blood Flow Metab* 24:62–66
18. Stevens MJ, Li F, Drel VR et al (2007) Nicotinamide reverses neurological and neurovascular deficits in streptozotocin diabetic rats. *J Pharmacol Exp Ther* 320:458–464
19. Bordone L, Motta MC, Picard F et al (2006) Sirt1 regulates insulin secretion by repressing UCP2 in pancreatic beta cells. *PLoS Biol* 4:e31
20. Ramsey KM, Mills KF, Satoh A, Imai S (2008) Age-associated loss of Sirt1-mediated enhancement of glucose-stimulated insulin secretion in beta cell-specific Sirt1-overexpressing (BESTO) mice. *Aging Cell* 7:78–88
21. Marcotte PA, Richardson PL, Guo J et al (2004) Fluorescence assay of SIRT protein deacetylases using an acetylated peptide substrate and a secondary trypsin reaction. *Anal Biochem* 332:90–99
22. Gale EA, Bingley PJ, Emmett CL, Collier T (2004) European Nicotinamide Diabetes Intervention Trial (ENDIT): a randomised controlled trial of intervention before the onset of type 1 diabetes. *Lancet* 363:925–931
23. Olmos PR, Hodgson MI, Maiz A et al (2006) Nicotinamide protected first-phase insulin response (FPIR) and prevented clinical disease in first-degree relatives of type-1 diabetics. *Diabetes Res Clin Pract* 71:320–333
24. de la Lastra CA, Villegas I, Sanchez-Fidalgo S (2007) Poly (ADP-ribose) polymerase inhibitors: new pharmacological functions and potential clinical implications. *Curr Pharm Des* 13:933–962
25. Gonzalez C, Menissier de Murcia J, Janiak P et al (2002) Unexpected sensitivity of nonobese diabetic mice with a disrupted poly(ADP-Ribose) polymerase-1 gene to streptozotocin-induced and spontaneous diabetes. *Diabetes* 51:1470–1476
26. Pieper AA, Brat DJ, Krug DK et al (1999) Poly(ADP-ribose) polymerase-deficient mice are protected from streptozotocin-induced diabetes. *Proc Natl Acad Sci U S A* 96:3059–3064
27. Drel VR, Lupachyk S, Shevalye H et al (2010) New therapeutic and biomarker discovery for peripheral diabetic neuropathy: PARP inhibitor, nitrotyrosine, and tumor necrosis factor- $\alpha$ . *Endocrinology* 151:2547–2555
28. Obrosova IG, Xu W, Lyzogubov VV et al (2008) PARP inhibition or gene deficiency counteracts intraepidermal nerve fiber loss and neuropathic pain in advanced diabetic neuropathy. *Free Radic Biol Med* 44:972–981
29. Onozaki A, Midorikawa S, Sanada H et al (2004) Rapid change of glucose concentration promotes mesangial cell proliferation via VEGF: inhibitory effects of thiazolidinedione. *Biochem Biophys Res Commun* 317:24–29
30. Zheng L, Szabo C, Kern TS (2004) Poly(ADP-ribose) polymerase is involved in the development of diabetic retinopathy via regulation of nuclear factor-kappaB. *Diabetes* 53:2960–2967
31. Boulton AJ (2004) The diabetic foot: from art to science. The 18th Camillo Golgi lecture. *Diabetologia* 47:1343–1353
32. Antonetti DA, Barber AJ, Bronson SK et al (2006) Diabetic retinopathy: seeing beyond glucose-induced microvascular disease. *Diabetes* 55:2401–2411
33. Virag L, Szabo C (2002) The therapeutic potential of poly(ADP-ribose) polymerase inhibitors. *Pharmacol Rev* 54:375–429
34. Obrosova IG, Li F, Abatan OI et al (2004) Role of poly(ADP-ribose) polymerase activation in diabetic neuropathy. *Diabetes* 53:711–720

35. Jagtap P, Szabo C (2005) Poly(ADP-ribose) polymerase and the therapeutic effects of its inhibitors. *Nat Rev Drug Discov* 4:421–440
36. Pacher P, Szabo C (2008) Role of the peroxynitrite-poly(ADP-ribose) polymerase pathway in human disease. *Am J Pathol* 173:2–13
37. Ha HC, Hester LD, Snyder SH (2002) Poly(ADP-ribose) polymerase-1 dependence of stress-induced transcription factors and associated gene expression in glia. *Proc Natl Acad Sci USA* 99:3270–3275
38. Minchenko AG, Stevens MJ, White L et al (2003) Diabetes-induced overexpression of endothelin-1 and endothelin receptors in the rat renal cortex is mediated via poly(ADP-ribose) polymerase activation. *FASEB J* 17:1514–1516
39. Du X, Matsumura T, Edelstein D et al (2003) Inhibition of GAPDH activity by poly(ADP-ribose) polymerase activates three major pathways of hyperglycemic damage in endothelial cells. *J Clin Invest* 112:1049–1057
40. Andrabi SA, Kim NS, Yu SW et al (2006) Poly(ADP-ribose) (PAR) polymer is a death signal. *Proc Natl Acad Sci USA* 103:18308–18313
41. Tissenbaum HA, Guarente L (2001) Increased dosage of a sir-2 gene extends lifespan in *Caenorhabditis elegans*. *Nature* 410:227–230
42. Canto C, Auwerx J (2009) Caloric restriction, SIRT1 and longevity. *Trends Endocrinol Metab* 20:325–331
43. Camins A, Sureda FX, Junyent F et al (2010) Sirtuin activators: designing molecules to extend life span. *Biochim Biophys Acta* 1799:740–749